INTERNATIONAL JOURNAL FOR NUMERICAL METHODS IN FLUIDS
Int. J. Numer. Meth. Fluids **31**: 1061–1085 (1999)

SOLUTION OF THE INCOMPRESSIBLE NAVIER–STOKES EQUATIONS ON DOMAINS WITH ONE OR SEVERAL OPEN BOUNDARIES[1]

F. BERTAGNOLIO[a,b,*]

[a] *Laboratoire d'Informatique pour la Mécanique et les Sciences de l'Ingénieur, BP 133, 91403 Orsay Cedex, France*
[b] *Risø National Laboratory, PO Box 49, DK-4000 Roskilde, Denmark*

SUMMARY

The aim of this paper is to develop a methodology for solving the incompressible Navier–Stokes equations in the presence of one or several open boundaries. A new set of open boundary conditions is first proposed. This has been developed in the context of the velocity–vorticity formulation, but it is also emphasized how it can be formally extended to the equations in primitive variables. The case of a domain involving several independent open boundaries is considered next. An influence matrix technique is applied such that the inlet mass flux is split onto the several outlets in order to enforce the prescribed mean pressure at each outlet. Both approaches are validated by numerical test cases. Copyright © 1999 John Wiley & Sons, Ltd.

KEY WORDS: open boundary; Navier–Stokes equations; incompressible flow; velocity–vorticity formulation

1. INTRODUCTION

Many practical problems in fluid dynamics are studied (or conceptualized) in unbounded domains. Obviously, these domains have to be truncated in order that the flow field can be computed on finite computational domains. As a consequence, boundary conditions (BCs) associated with these so-called 'open' boundaries are to be defined. The ability of these latter conditions to correctly represent the real unbounded domain is crucial for the accuracy of the computed flow field, especially when those boundaries are located in the vicinity of the regions where the phenomena of interest occur. Furthermore, particularly in the context of an incompressible fluid, these conditions may greatly influence the flow inside the computational domain, since any error on the flow field (say at the boundary) is instantaneously felt in the whole domain.

Defining such open boundary conditions (OBCs) is a difficult task. Indeed, they partly depend on the flow outside the computational domain, which is logically unknown. Thus, one has to introduce artificial BCs that may contain some additional information to be defined. Whatever these conditions are, the numerical problem to be solved must be mathematically well posed. Usual BCs for the Navier–Stokes equations consist of Dirichlet BCs for both

* Correspondence to: Wind Energy and Atmospheric Physics Department, Building VEA-762, Risø National Laboratory, PO Box 49, DK-4000 Roskilde, Denmark. E-mail: franck.bertagnolio@risoe.dk

[1] Some of the results in this article were presented at the 10th International Conference on Numerical Methods for Laminar and Turbulent Flows [1].

CCC 0271–2091/99/231061–25$17.50

Received 18 June 1998
Revised 18 December 1998

velocity components normal and tangent to the boundary. In the context of an incompressible flow for which a pressure equation can be derived by combining momentum equation and the divergence-free condition, the definition of the normal velocity component yields a Neumann BC for the resulting Poisson problem. However, when dealing with open boundaries on which the velocity components are unknown, one usually has to resort to other BCs.

The homogeneous Neumann BC is commonly used as a passive condition at the open boundaries. However, since we are concerned with the normal momentum equation at the boundary, this condition applied to the normal velocity component yields an ill-posed problem [2]. Moreover (or consequently?), this homogeneous Neumann BC has been known to give poor results for high Reynolds numbers [3,4], and therefore the boundaries have to be located far away from the area of interest, increasing the computing time of the numerical model. Some authors also derive OBCs based on the stress tensor (see the discussion by Gresho [5]). In this case, the problem is mathematically well posed, but this tensor is once again unknown and a zero stress condition is usually assumed [2]. Furthermore, the methodology by Bruneau and Fabrie [6], for which the stress tensor is derived from a reference flow, is also of interest. This kind of OBC naturally yields Dirichlet BCs for the pressure, and usually results in good behaviour. However, the strong coupling between the pressure and the velocity due to incompressibility is also a source of difficulty at the boundaries. For an exhaustive overview of the different OBCs, the reader is referred to the review papers by Sani and Gresho [2] and Gresho [5].

In contrast, the velocity–vorticity formulation of the Navier–Stokes equations has gained some favour thanks to its ability to decouple the dynamic feature (momentum conservation equation) from the kinematics (see further). Indeed, by taking the curl of the momentum equation, the pressure no longer appears in the subsequent vorticity transport equation. Consequently, in the case of flows with open boundaries, the BCs for the vorticity are easier to implement than those for the velocity. Nevertheless, BCs for the velocity are still required when solving the kinematic equations.

This paper first attempts to clarify the definition of such OBCs in the context of the velocity–vorticity formulation. A new set of BCs resulting in a well-posed problem is defined. This will be proven to remain efficient, even for short domains. Moreover, it will be shown that the foreseen advantages involved with this formulation can be extended to the equations in primitive variables, as long as both formulations are readily equivalent. The key points of our approach are (1) to benefit from the easy implementation of the BCs for the vorticity transport equation and (2) to use the natural Dirichlet BCs for the normal velocity component in the course of the kinematic problem, such that it is well posed. This normal component will be derived from an advection–diffusion equation for an additional unknown. Such a methodology was proposed by the author at the *10th International Conference on Numerical Methods for Laminar and Turbulent Flows* that held in Swansea [1]. The results that had then been obtained are greatly improved herein. Subsequently, it is proven that this methodology is an attractive alternative to the usual OBCs.

The treatment of multiple open boundaries is also a major difficulty. Indeed, one has to determine how the inlet mass flux is split onto these several open boundaries. Actually, the outlet fluxes depend on the flow outside the computational domain (which is unknown, as mentioned earlier). By using a weak formulation of the Navier–Stokes equations, Heywood *et al.* [7] show that a natural way to handle this case is to enforce the mean pressure at each boundary. In a similar manner, a technique that consists of defining the net mass flux across each outlet boundary such that the prescribed mean pressures are enforced is introduced. It is based on the previous mentioned methodology for defining the OBCs.

The paper is organized as follows. The Navier–Stokes equations are first recalled, and the velocity–vorticity formulation is introduced. The implementation of the BCs such that both formulations are readily equivalent is emphasized. BCs for a single open boundary are defined in Section 4 and numerically tested. Finally, the case of multiple open boundaries is considered. Comments on the extension of both methodologies to the equations in primitive variables are given in Section 7.

2. GOVERNING EQUATIONS

Let us consider the flow of an incompressible viscous fluid in a domain Ω bounded by Γ. It is assumed that there exists N surface pieces $\{\Gamma_i\}_{i=1,\ldots,N}$ lying on Γ at the intersection of Ω and the flow field region outside Ω. The velocity (and all flow-related quantities) on these surfaces Γ_i is naturally part of the unknowns. The Γ_i will be hereafter denoted by open boundaries as opposed to the other boundary parts, such as inlets or walls, on which the velocity flow field is assumed to be known.

The non-dimensional Navier–Stokes equations in primitive variables are, in rotational form,

$$\frac{\partial \boldsymbol{v}}{\partial t} + \boldsymbol{w} \times \boldsymbol{v} = -\nabla p_t - \frac{1}{Re} \nabla \times \boldsymbol{w} \quad \text{in } \Omega, \tag{1}$$

$$\nabla \cdot \boldsymbol{v} = 0 \quad \text{in } \Omega, \tag{2}$$

where $\boldsymbol{v}$ is the velocity and the vorticity $\boldsymbol{w}$ is defined as the curl of the velocity, Re is the Reynolds number and the dynamic pressure p_t is related to the static pressure p through the following relation:

$$p_t = p + \frac{1}{2}\boldsymbol{v}^2.$$

On the boundaries, both normal and tangential components of the velocity are usually prescribed

$$\boldsymbol{v} \cdot \boldsymbol{n} = \boldsymbol{b} \cdot \boldsymbol{n} \quad \text{on } \Gamma, \tag{3}$$

$$\boldsymbol{v} \times \boldsymbol{n} = \boldsymbol{b} \times \boldsymbol{n} \quad \text{on } \Gamma, \tag{4}$$

where $\boldsymbol{n}$ denotes the unit outer vector normal to the boundary Γ. The prescribed boundary velocity $\boldsymbol{b}$ has to satisfy the following compatibility constraint:

$$\iint_\Gamma \boldsymbol{b} \cdot \boldsymbol{n} \, \mathrm{d}\Gamma = 0, \tag{5}$$

in accordance with the divergence-free condition (2). Together with the definition of an initial solenoidal velocity field, Equations (1)–(5) are well posed (see Gresho [5]). But, as mentioned earlier, the boundary velocity field $\boldsymbol{b}$ is usually unknown on the boundary parts $\{\Gamma_i\}_{i=1,\ldots,N}$. The aim of this paper is to define some appropriate numerical procedure for computing those values, both in the case of a single open boundary ($N=1$) and multiple open boundaries ($N \geq 2$).

For the sake of simplicity, the following right-handed orthonormal vector basis ($\boldsymbol{t}_1$, $\boldsymbol{t}_2$, $\boldsymbol{n}$), for which $\boldsymbol{t}_1$ and $\boldsymbol{t}_2$ are tangent to the boundary, is introduced on Γ. The projection of any vector field $\boldsymbol{a}$ onto the plane tangent to the boundary thus reads as

$$\boldsymbol{a} \times \boldsymbol{n} = a_{t_1}\boldsymbol{t}_1 + a_{t_2}\boldsymbol{t}_2.$$

3. VELOCITY–VORTICITY FORMULATION

The velocity–vorticity (hereafter denoted by $\boldsymbol{v}$–$\boldsymbol{w}$) formulation of the Navier–Stokes equations has been seen by several authors as an attractive alternative to the equations in primitive variables. Particularly, it seems that the implementation of BCs on open boundaries is more straightforward [8–10]. It will be shown below that this is not obvious, since both formulations are equivalent.

In this section, the equivalence of the formulations is addressed and the $\boldsymbol{v}$–$\boldsymbol{w}$ formulation is shown to be a particular fractional step method, as stated by Lardat *et al*. [11]. The treatment of the BCs is emphasized.

3.1. Set of $\boldsymbol{v}$–$\boldsymbol{w}$ equations

By taking the curl of Equation (1), it can be proven (see Daube *et al*. [12]) that the primitive form of the Navier–Stokes equations (1)–(4) is equivalent to the so-called $\boldsymbol{v}$–$\boldsymbol{w}$ formulation

$$\frac{\partial \boldsymbol{w}}{\partial t} + \nabla \times (\boldsymbol{w} \times \boldsymbol{v}) = \frac{1}{Re} \nabla \times (\nabla \times \boldsymbol{w}) \quad \text{in } \Omega, \tag{6}$$

$$\nabla \times \boldsymbol{v} = \boldsymbol{w} \quad \text{in } \Omega, \tag{7}$$

$$\nabla \cdot \boldsymbol{v} = 0 \quad \text{in } \Omega, \tag{8}$$

$$\boldsymbol{v} \cdot \boldsymbol{n} = \boldsymbol{b} \cdot \boldsymbol{n} \quad \text{on } \Gamma, \tag{9}$$

$$\boldsymbol{v} \times \boldsymbol{n} = \boldsymbol{b} \times \boldsymbol{n} \quad \text{on } \Gamma, \tag{10}$$

which is always subject to the compatibility constraint (5). If the domain Ω is p multiply connected, p additional conditions ensuring that the pressure is uniform in the domain arise [12]. Without loss of generality, the domain is hereafter assumed to be simply connected.

The solution procedure for this new set of equations always reduces to a two-step problem:

1. Solve the convection–diffusion equation (6) for the vorticity $\boldsymbol{w}$ with appropriate BCs that will be discussed below.
2. Solve the so-called div–curl problem (7)–(9), which consists of finding the divergence-free velocity field $\boldsymbol{v}$ whose curl is the vorticity $\boldsymbol{w}$ and for which the normal component on the boundary is known.

Notice that there is no explicit BC on the vorticity when solving Equation (6), except its definition as the curl of the velocity (Equation (7)). However, the velocity depends on the vorticity itself through the div–curl problem. Actually, there exists an integral condition (see Dennis and Quartapelle [13]) so that the tangential components of the vorticity along the boundary must be estimated in the first step of the solution procedure such that Equation (10) is satisfied at the end of the second step. This coupling may be achieved either by means of an influence matrix technique [14], or in a decoupled manner by approximating the boundary vorticity in the first step [15].

3.2. Link with a fractional step method

By introducing a Helmholtz-type decomposition of the velocity flow field for solving the div–curl problem [16], it has been shown by Lardat *et al.* [11] that such a method is readily equivalent to a fractional step method for solving the Navier–Stokes equations in primitive variables. The procedure is briefly described below.

Let us assume that Equation (6) has been discretized with respect to time by making use of any temporal scheme. In this case, the time derivative is approximated by a second-order backward temporal scheme. Viscous terms are treated implicitly, whereas convective terms are evaluated using a second-order accurate-in-time Adams–Bashforth extrapolation. The vorticity transport equation is thus

$$\frac{3\boldsymbol{w}^{n+1}-4\boldsymbol{w}^{n}+\boldsymbol{w}^{n-1}}{2\,\Delta t}+\nabla\times(\boldsymbol{w}\times\boldsymbol{v})^{*}=\frac{1}{Re}\,\nabla\times\nabla\times\boldsymbol{w}^{n+1}, \tag{11}$$

where $n+1$, n and $n-1$ denote the successive time levels, Δt is the time step and the asterisk denotes the Adams–Bashforth extrapolation. Thanks to the rotational form of the convective and viscous terms, the solution method only requires the tangential vorticity components as BCs. These components are stated as described in Subsection 3.1.

After solving the previous equation, all its terms are known. Then let the 'predicted' velocity vector field $\tilde{\boldsymbol{v}}$ be explicitly defined such that

$$\frac{3\tilde{\boldsymbol{v}}-4\boldsymbol{v}^{n}+\boldsymbol{v}^{n-1}}{2\,\Delta t}+(\boldsymbol{w}\times\boldsymbol{v})^{*}=-\frac{1}{Re}\,\nabla\times\boldsymbol{w}^{n+1}. \tag{12}$$

Notice that the component of $\tilde{\boldsymbol{v}}$ normal to the boundary is defined by projecting Equation (12) onto the normal $\boldsymbol{n}$. Hence, the tangential components of $\tilde{\boldsymbol{v}}$ satisfy Neumann BCs by definition of the vorticity components tangent to the boundary

$$\frac{\partial\tilde{v}_{t_1}}{\partial n}=+w_{t_2}+\frac{\partial\tilde{\boldsymbol{v}}\cdot\boldsymbol{n}}{\partial t_1}\quad\text{on }\Gamma, \tag{13}$$

$$\frac{\partial\tilde{v}_{t_2}}{\partial n}=-w_{t_1}+\frac{\partial\tilde{\boldsymbol{v}}\cdot\boldsymbol{n}}{\partial t_2}\quad\text{on }\Gamma. \tag{14}$$

The predicted velocity field is now projected onto the space of divergence-free vector field by adding the gradient of some scalar function ϕ, such that

$$\frac{3}{2\,\Delta t}\,(\boldsymbol{v}^{n+1}-\tilde{\boldsymbol{v}})=-\nabla\phi. \tag{15}$$

The scalar function equation originates from the divergence-free condition (8) supplemented by BCs derived from (9). Indeed, taking the divergence of the previous equation yields the following Poisson problem:

$$\nabla^{2}\phi=\frac{3}{2\,\Delta t}\,\nabla\cdot\tilde{\boldsymbol{v}}\quad\text{in }\Omega, \tag{16}$$

$$\nabla\phi\cdot\boldsymbol{n}=\frac{3}{2\,\Delta t}\,(\tilde{\boldsymbol{v}}\cdot\boldsymbol{n}-\boldsymbol{b}\cdot\boldsymbol{n})\quad\text{on }\Gamma, \tag{17}$$

for which the solution exists and is unique provided that Equation (5) is satisfied. Incorporating Equation (15) into Equation (12) yields Equation (1), and ϕ corresponds to the dynamic pressure p_t itself. This solution procedure can be extended for solving the three-dimensional

Navier–Stokes equations on non-orthogonal curvilinear MAC grids as described previously by the author [16,17].

It is emphasized that it would be readily equivalent to solve the equation in primitive variables by means of the fractional step method, which consists of: first solve Equations (12)–(14) to obtain the predicted velocity $\tilde{\boldsymbol{v}}$ (predictor step); then solve the Poisson problem (16) and (17) for the dynamic pressure p_t (corrector step).

3.3. Comments on the boundary conditions

It must be pointed out that the proposed method mainly differs from the usual fractional step methods insofar as here it implicitly makes use of Neumann BCs, (13) and (14), for the tangential components of the velocity. The normal velocity component $\tilde{\boldsymbol{v}}\cdot\boldsymbol{n}$ has been given by projecting (12) onto the normal $\boldsymbol{n}$. The equivalence between the $\boldsymbol{v}$–$\boldsymbol{w}$ formulation and the fractional step method is thus ensured only for those particular BCs. In contrast, fractional step methods usually make use of Dirichlet BCs for the tangential components of the predicted velocity

$$\tilde{\boldsymbol{v}}\times\boldsymbol{n}=\boldsymbol{b}\times\boldsymbol{n} \quad \text{on } \Gamma.$$

To sum up, whether the $\boldsymbol{v}$–$\boldsymbol{w}$ formulation or the equivalent fractional step method is used, the solution algorithm consists of the two steps:

1. A 'dynamic' problem for the vorticity $\boldsymbol{w}$ or the predicted velocity $\tilde{\boldsymbol{v}}$ respectively requires Dirichlet BCs for the vorticity components tangent to the boundary, or equivalently, Neumann BCs for $\tilde{\boldsymbol{v}}\times\boldsymbol{n}$.
2. A 'kinematic' problem in form of a Poisson equation requires the value of the velocity component normal to the boundary $\boldsymbol{b}\cdot\boldsymbol{n}$.

On a wall, the tangential vorticity component adjusts itself (see above) in order to satisfy the BC (10). In a similar manner, on an inlet, the vorticity distribution can be calculated in order to enforce any prescribed tangential velocity, or it can be assigned to any desired value (zero for instance). On both inlets and walls, the normal velocity component is assumed to be known. More precisely, it is given by the inlet mass flux on the inlets, and it is zero on walls. On the open boundaries, neither the tangential vorticity components nor the normal velocity component are known. The difficulty lies in the definition of those quantities. In the following, we focus on the $\boldsymbol{v}$–$\boldsymbol{w}$ formulation. The fractional step method will be discussed at the end of this paper.

4. SINGLE OPEN BOUNDARY

In this section, it is first assumed that there exists only one open boundary part Γ_1 on which the flow is unknown (i.e. $N=1$, see Section 2). Determination of the OBCs for the dynamic and for the kinematic problems is described. This procedure was originally reported by the author [1]. First, the vorticity transport equation is used for deriving BCs for the vorticity. Then the Dirichlet BC for the normal velocity component required for solving the kinematic problem is derived such that the compatibility constraint is ensured. This normal component is computed by solving an additional advection–diffusion equation for its own derivative along the boundary. The present procedure is improved compared with the one presented at Swansea [1].

4.1. *Dynamic open boundary condition*

As mentioned before, the solution of the dynamic problem requires the values of the vorticity components tangent to the boundary. If the open boundary is far away from walls, viscous effects may be neglected and an extrapolation of the values through a particle method may be used (see Ta Phuoc and Bouard [8]). This, in the two-dimensional case, is

$$\frac{\mathrm{D}(\boldsymbol{w} \times \boldsymbol{n})}{\mathrm{D}t} = 0,$$

and means that the actual vorticity on the boundary is assigned by using its value at the location of the actual fluid particle at the previous time level. This approach was used by the author in the previous mentioned work [1] and will be denoted hereafter as the 'particle method'. Notice that in the three-dimensional case, the stretching term of the vorticity transport equation should be added.

In the vicinity of walls, it is well known that the particle method is a poor approximation. The convection–diffusion equation (6) projected onto the plane tangent to the open boundary surface may alternatively be solved in order to compute the tangential components of the vorticity [9]. This approach will be preferred and used in this paper. The spatial discretization of this equation introduces quantities outside the computational domain, both through the diffusive and the convective terms. The former difficulty is solved by neglecting the diffusion normal to the boundary. This is equivalent to the following homogeneous Neumann BC:

$$\frac{\partial}{\partial n}\left[(\nabla \times \boldsymbol{w}) \times \boldsymbol{n}\right] = 0.$$

Concerning the convective term, a first-order accurate upwind scheme is used, avoiding the value of the vorticity outside the computational domain. In the end, the actual equation is very similar to the so-called 'advective derivative condition', which is often used to derive unknown values on the open boundaries [2]. It is here applied to compute the vorticity.

4.2. *Kinematic open boundary condition*

In the second solution step, the velocity component normal to the boundary has to be defined. Owing to the fact that the compatibility constraint (5) must be ensured, the assignment of this value is crucial. Notice that the normal velocity component is the integral of its own derivative along the boundary which is just the vorticity by adding the normal derivative of a tangential velocity component (Equations (13) and (14)). If these last quantities are known, the normal component can thus be recovered by using a simple spatial integration.

4.2.1. Two-dimensional case. For the sake of simplicity, let us first consider the two-dimensional flow in the Cartesian plane (x, y) such that the open boundary Γ_1 is a line $x = \text{constant}$. Let u and v denote the x and y components of the velocity respectively. Also, the vorticity reduces to a scalar field hereafter denoted by w. The mass flux across an elementary surface $\mathrm{d}\Gamma$ of the open boundary is a function of y

$$\boldsymbol{v} \cdot \boldsymbol{n} \, \mathrm{d}\Gamma = u(y) \, \mathrm{d}\Gamma,$$

where $\mathrm{d}\Gamma = \mathrm{d}y$ in this case. Assume that the value of $\partial u/\partial y$ is known on the open boundary (the computation of this quantity will be addressed later in Section 4.3). Integration along the boundary then yields

$$u(y) = \int_0^y \frac{\partial u}{\partial y}(\tilde{y})\,\mathrm{d}\tilde{y} + u(0), \tag{18}$$

where $y = 0$ denotes any point on the open boundary Γ_1. Let this point be one of the ends of the boundary, and let $y = L$ denote the other end. The mass flux across Γ_1 is

$$\int_0^L \boldsymbol{v}\cdot\boldsymbol{n}\,\mathrm{d}\Gamma = \int_0^L \left(\int_0^y \frac{\partial u}{\partial y}(\tilde{y})\,\mathrm{d}\tilde{y} + u(0)\right)\mathrm{d}y,$$

and it has to match the inlet mass flux D_{in}, which is assumed known. After some simple algebra, we get

$$u(0) = \left(D_{\mathrm{in}} - \int_0^L \left(\int_0^y \frac{\partial u}{\partial y}(\tilde{y})\,\mathrm{d}\tilde{y}\right)\mathrm{d}y\right) \Big/ \int_0^L \mathrm{d}y.$$

The normal velocity component on Γ_1 can now be recovered thanks to Equation (18).

This methodology of calculating the velocity component normal to the boundary presents some advantages. First, the easily computed single constant $u(0)$ adjusts itself in order to ensure the compatibility constraint (5). Moreover, this constraint is satisfied identically; remember that it is a necessary condition for the div–curl (or the Poisson) problem to have a solution. Finally, the choice of the location $y = 0$ is arbitrary since the normal velocity component is uniquely defined by its derivative and the value of its integral along the boundary.

In the paper by Sani and Gresho [2], a similar technique also yields the computation of a single constant, which allows the compatibility constraint to be satisfied. In addition, the homogeneous Neumann BC

$$\frac{\partial \boldsymbol{v}}{\partial x} = 0$$

is used based on the assumption of fully developed flow, an assumption that is not always justified.

4.2.2. Three-dimensional case. The above-described procedure is now extended to the general three-dimensional case. Let $\boldsymbol{x}_1$ denote the spatial variable on the open boundary Γ_1, and $\boldsymbol{x}_{1,0}$ any particular point on this surface. In the same way as in the two-dimensional case, the normal velocity component can be obtained by integrating its own derivative, i.e.

$$\boldsymbol{b}\cdot\boldsymbol{n}(\boldsymbol{x}_1) = \int_{\gamma(\boldsymbol{x}_1)} \left[\frac{\partial \boldsymbol{v}\cdot\boldsymbol{n}}{\partial \gamma}(\boldsymbol{x}_1)\right]\mathrm{d}\gamma + \boldsymbol{b}\cdot\boldsymbol{n}(\boldsymbol{x}_{1,0}),$$

where $\gamma(\boldsymbol{x}_1)$ denotes any path lying on the surface Γ_1 and joining $\boldsymbol{x}_{1,0}$ to $\boldsymbol{x}_1$, and $\mathrm{d}\gamma$ denotes an elementary curve length along this path. The following notation is introduced:

$$B_1(\boldsymbol{x}_1) \equiv \int_{\gamma(\boldsymbol{x}_1)} \left[\frac{\partial \boldsymbol{v}\cdot\boldsymbol{n}}{\partial \gamma}(\boldsymbol{x}_1)\right]\mathrm{d}\gamma.$$

The definition of the normal velocity component on Γ_1 proceeds as in the previous section. Namely, the constant $\boldsymbol{b}\cdot\boldsymbol{n}(\boldsymbol{x}_{1,0})$ is computed by making use of the inlet mass flux, then the normal velocity component is recovered by integrating the former equation.

It is noteworthy that the boundary scalar field $\boldsymbol{b}\cdot\boldsymbol{n}(\boldsymbol{x}_1)$ should be independent on the path $\gamma(\boldsymbol{x}_1)$ chosen for integration. Based on this, the integrated quantity would have to satisfy the following compatibility constraint:

$$\oint_{\gamma_c} \left[\frac{\partial \boldsymbol{v} \cdot \boldsymbol{n}}{\partial \gamma} (\boldsymbol{x}_1) \right] \mathrm{d}\gamma = 0,$$

for any loop γ_c lying on Γ_1. However, this last condition has not been ensured in the three-dimensional calculations presented later.

4.3. Derivative of the velocity component on the open boundary

As stated in the two previous subsections, the values of the tangential derivatives of the normal velocity component on the open boundary have to be estimated. At this point of the numerical procedure, the tangential components of the vorticity on the boundary have already been computed. The searched quantities are then directly related to the normal derivatives of the tangential velocity components through Equations (13) and (14). Owing to the fact that far away from the region of interest, the flow is roughly constant, homogeneous Neumann BC for the unknowns may be assumed [8]

$$\frac{\partial v_{t_1}}{\partial n} = 0, \qquad \frac{\partial v_{t_2}}{\partial n} = 0. \tag{19}$$

However, it has been shown [1] that this kind of BC yields unrealistic numerical behaviour when vortex structures are going across the open boundary if the mesh is not adapted (say if the mesh is too short). An improved condition has, therefore, been proposed. Instead of arbitrarily assigning this value to zero, the author suggested that it can be carried out with the fluid particles [1], as done for the vorticity

$$\frac{\mathrm{D}}{\mathrm{D}t}\left(\frac{\partial v_{t_1}}{\partial n}\right) = 0, \qquad \frac{\mathrm{D}}{\mathrm{D}t}\left(\frac{\partial v_{t_2}}{\partial n}\right) = 0. \tag{20}$$

These last equations can actually be derived from the momentum equation. In addition to viscous effects, the pressure gradient has been neglected since the projection of the Euler equation onto the direction tangential to the boundary reads

$$\frac{\mathrm{D}(\boldsymbol{v} \times \boldsymbol{n})}{\mathrm{D}t} = -(\nabla p) \times \boldsymbol{n}.$$

Equations (20) then omit the cross-derivative of the pressure. Nevertheless, these BCs present better results than the homogeneous Neumann BCs [1].

In the current paper, it is proposed to derive a convection–diffusion equation for the searched quantities in the same spirit as in the paper by Jin and Braza [18]. In their work, a non-reflecting OBC for the velocity vector field was derived from a wave equation (see the work by Engquist and Majda [19]). In the current case, the same technique is applied to the tangential derivatives of the normal velocity. Thereby, the following equations can be obtained:

$$\frac{\partial}{\partial t}\left(\frac{\partial \boldsymbol{v} \cdot \boldsymbol{n}}{\partial t_j}\right) + (\boldsymbol{v} \cdot \boldsymbol{n}) \frac{\partial}{\partial n}\left(\frac{\partial \boldsymbol{v} \cdot \boldsymbol{n}}{\partial t_j}\right) = +\frac{1}{Re}\left(\frac{\partial^2}{\partial t_1^2} + \frac{\partial^2}{\partial t_2^2}\right)\left(\frac{\partial \boldsymbol{v} \cdot \boldsymbol{n}}{\partial t_j}\right) \quad \text{on } \Gamma_1, \tag{21}$$

for $j = 1, 2$. In the two-dimensional case and with the notations introduced above, this equation reduces to

$$\frac{\partial}{\partial t}\left(\frac{\partial u}{\partial y}\right) + u \frac{\partial}{\partial x}\left(\frac{\partial u}{\partial y}\right) = +\frac{1}{Re}\frac{\partial^2}{\partial y^2}\left(\frac{\partial u}{\partial y}\right) \quad \text{on } \Gamma_1. \tag{22}$$

The discretization scheme used for the unsteady term is the same as the one used for the vorticity transport equation (see Section 3.2). The viscous term is treated implicitly by making use of a classical central difference scheme second-order accurate in space. Concerning the convective term, an additional difficulty arises owing to the fact that any equation for the unknown quantities is solved inside the computational domain. Therefore, the convective term is discretized with respect to an explicit-in-time Beam–Warming upwind scheme.

4.4. Numerical results

In order to test the current OBCs, the two-dimensional flow over a circular cylinder has been computed in several configurations. Six different computational grids denoted by M1–M6 are used. The open boundaries are respectively located at 19.9, 14.6, 12.0, 6.7, 5.4 and 4.0 cylinder diameters downstream from the centre of the cylinder.

The first test case is the impulsively started cylinder with a steady state Reynolds number based on the cylinder diameter and the velocity at infinity equal to $Re = 40$. The growth of the separation bubble is compared with the experimental results by Coutanceau and Bouard [20] and the numerical ones by Collins and Dennis [21]. The results obtained with the present method are presented for the computation on the longest mesh M1 and on the three shortest meshes M4, M5 and M6 in Figure 1. A good agreement between these computed results and those from the literature is observed, except for the shortest mesh M6, which is obviously too short to capture the phenomenon correctly.

The two next test cases concern the unsteady flow around the cylinder for a Reynolds number set equal to $Re = 200$ and $Re = 1000$ respectively. During the first time of the computation ($t < 5$), several abrupt circular motions of the cylinder are enforced in order to destabilize the flow, rapidly yielding a von Karmann vortex street downstream the cylinder.

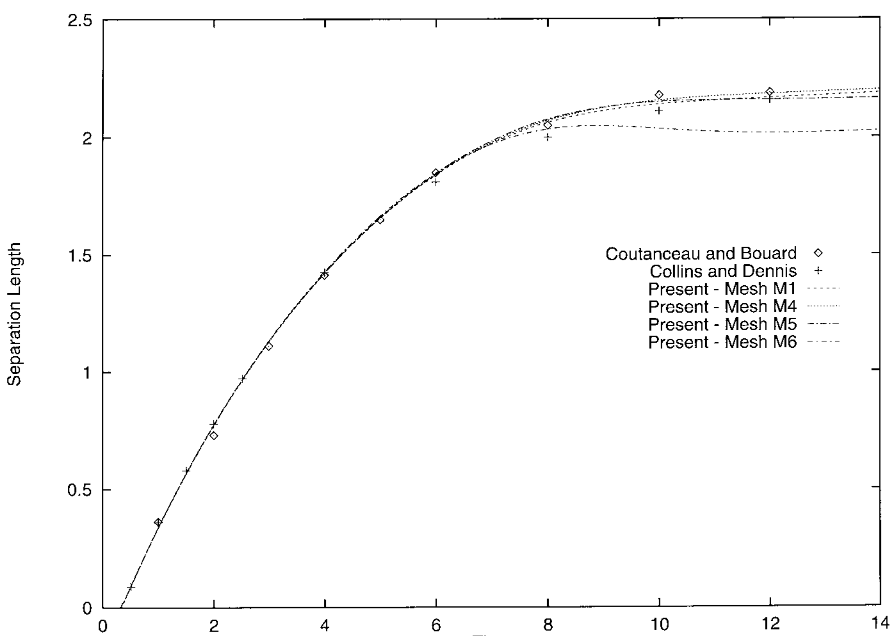

Figure 1. Development of the separation bubble behind the cylinder, $Re = 40$.

Table I. Comparison of results for unsteady flow over a cylinder, $Re = 200$

Reference	Drag coefficient	Strouhal number
Present, mesh M1	1.373	0.1988
Present, mesh M2	1.375	0.1989
Present, mesh M3	1.374	0.1989
Present, mesh M4	1.380	0.1995
Liu *et al.* [22]	1.31	0.192
Belov *et al.* [a]	1.19	0.193
Rogers *et al.* [b]	1.23	0.185
Miyake *et al.* [a]	1.34	0.196
Rosenfeld *et al.* [b]	1.46	0.211
Lecointe *et al.* [a]	1.58	0.194
Lin *et al.* [a]	1.17	
Henderson *et al.* [a]		0.197
Kovaznay (exp.) [b]		0.19
Roshko (exp.) [b]		0.19
Williamson (exp.) [a]		0.197
Wille (exp.) [b]	1.3	

[a] These results are collected in papers by Belov *et al.*, which are in turn cited in Reference [22].
[b] These results are collected in papers by Rogers *et al.*, which are in turn cited in Reference [22].

The results obtained for the case $Re = 200$ are first compared with data from the literature. The computed Strouhal number and mean drag coefficient are presented in Table I, also showing the results of Liu *et al.* [22] and those by Belov *et al.* and Rogers *et al.* that are cited in Reference [22]. The results obtained with the present method are very close to each other

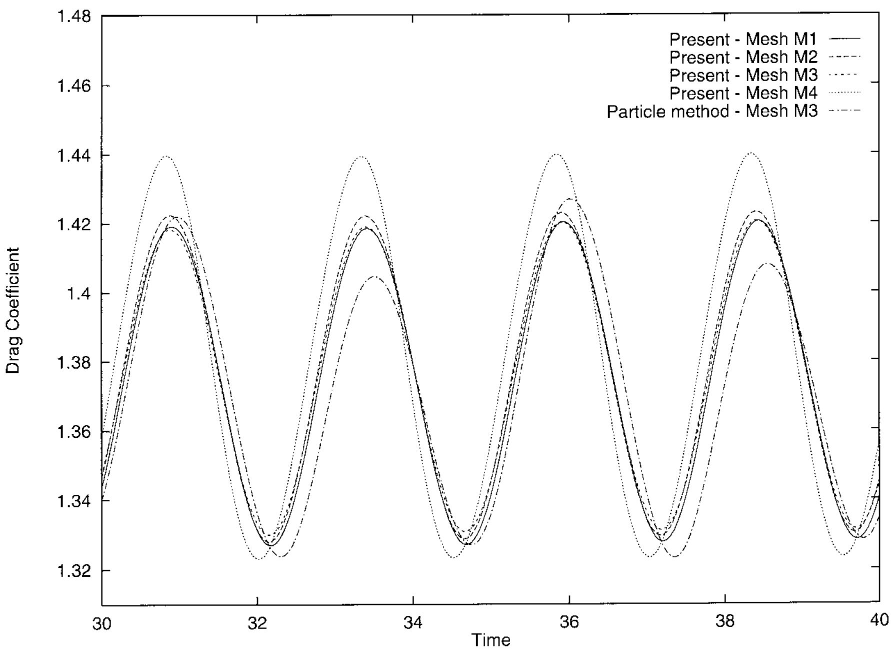

Figure 2. Time series of the drag coefficient, $Re = 200$.

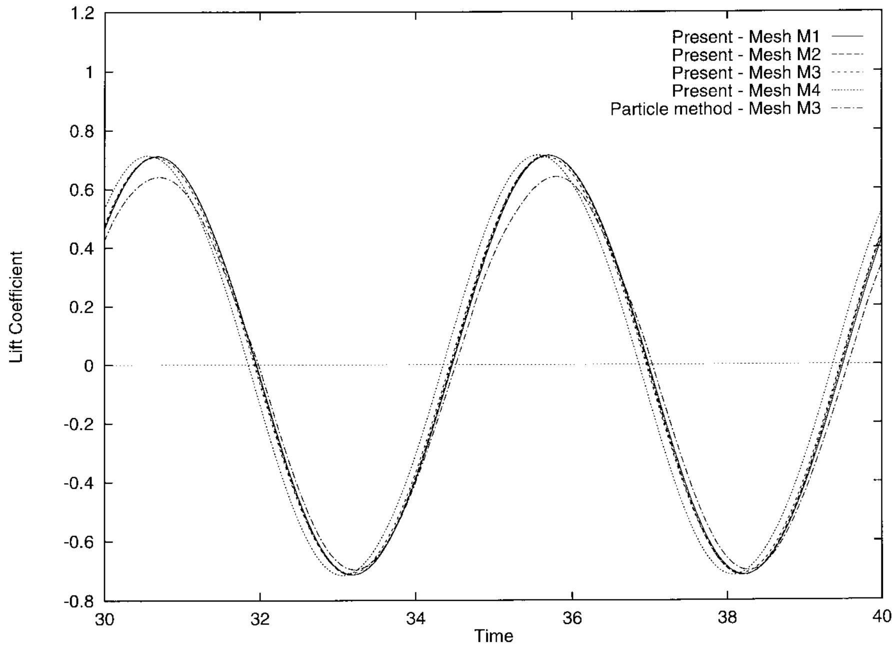

Figure 3. Time series of the lift coefficient, $Re = 200$.

and match with the other results available in the literature. As expected, the results deteriorate when the mesh is getting shorter. Namely, the drag coefficient and the Strouhal number are increasingly perceptible for the mesh M4.

The time series of the drag and lift coefficients are reported in Figures 2 and 3 respectively for $Re = 200$, and in Figures 4 and 5 for $Re = 1000$, for a dimensionless time $30 < t < 40$ for which a periodic state has been reached. It can be seen that the lift coefficient is almost non-sensitive to the mesh extension. The drag coefficient is a bit more sensitive and discrepancies in the results arise for the shortest mesh considered, mesh M4. However, good agreement is found between the three other meshes. The results obtained with the particle method [1] on mesh M3 are also reported in these figures. The present approach yields better results both for the drag and lift coefficients, even for the shortest mesh, mesh M4, so far as the particle method does not allow for a fully periodic state to be reached.

The isovalues of the computed vorticity and dynamic pressure at the dimensionless time $t = 40$ are finally presented for the case of $Re = 1000$ with the present method. Since the open boundary of mesh M2 is far away from the cylinder, the flow field in the place of the open boundaries of the shorter meshes should be independent of the OBCs. It is consequently a good approximation of the real unbounded flow at these places. Indeed, the isovalues of the vorticity on meshes M3 and M4 exhibit little discrepancies with mesh M2 (see Figure 6). The pressure is a very sensitive quantity, which is scarcely reported by the authors when testing OBCs. In the current case, a relatively good agreement is found between the different meshes (Figure 7). However, a slight suction phenomenon of the vortex structures in the vicinity of the open boundaries of the shortest meshes can be observed when the isovalues are compared with those on the longer mesh.

5. SEVERAL OPEN BOUNDARIES

The case for which the number of the open boundary parts is larger than one (i.e. $N \geq 2$, see Section 2) is now considered. The procedure for defining the BCs described in the previous section can be applied on each boundary part Γ_i. In addition to the evaluation of the tangential components of the vorticity and the tangential derivatives of the normal velocity component, N scalar unknowns arise with the definition of the mass fluxes across each open boundary (see Section 4.2). However, the compatibility constraint yields a single equation. The goal of this section is to determine how the inlet mass flux is split onto the several open boundaries.

5.1. Defining the additional conditions

Hereafter, $\boldsymbol{x}_i$ denotes the spatial variable on the open boundary part Γ_i ($i = 1, \ldots, N$) and $B_i(\boldsymbol{x}_i)$ denotes the integral as defined in Section 4.2.2 for any path $\gamma(\boldsymbol{x}_i)$ lying on Γ_i. The N scalar unknowns arising with the mass fluxes across each boundary part Γ_i are $\boldsymbol{b} \cdot \boldsymbol{n}(\boldsymbol{x}_{i,0})$, where $\boldsymbol{x}_{i,0}$ denotes any location on Γ_i.

As previously described, the computation of the BCs on each open boundary Γ_i reduces to:

- compute the tangential components of the vorticity $\boldsymbol{w} \times \boldsymbol{n}$ and the tangential derivatives of the normal velocity component $\partial \boldsymbol{v} \cdot \boldsymbol{n} / \partial t_j$ ($j = 1, 2$);
- determine the normal component of the velocity $\boldsymbol{b} \cdot \boldsymbol{n}$ ($j = 1, 2$).

The solution of the first step has already been discussed in the previous section. Concerning the second step, it has also been described how the normal velocity component can be computed on each open boundary Γ_i (see Section 4.2.2) as

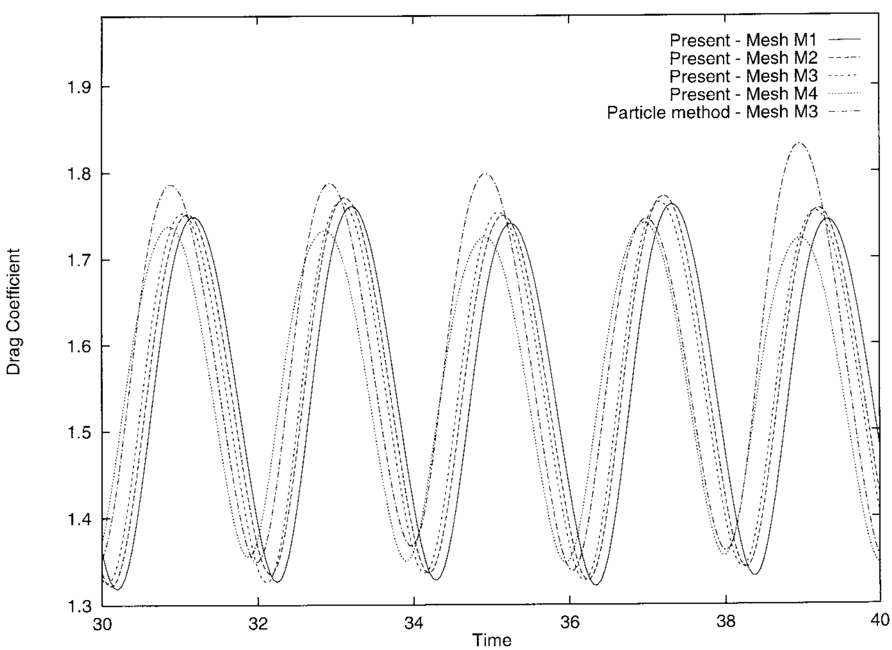

Figure 4. Time series of the drag coefficient, $Re = 1000$.

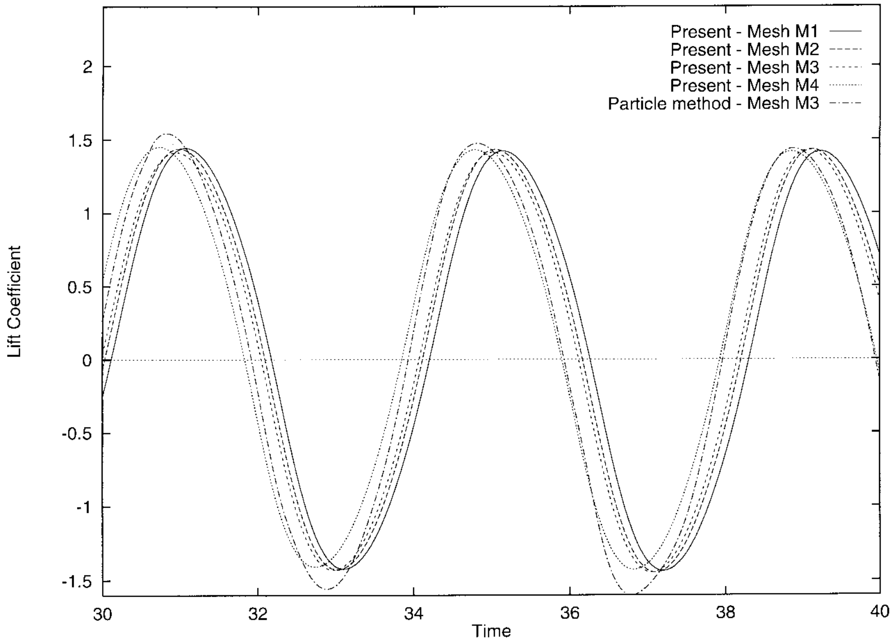

Figure 5. Time series of the lift coefficient, $Re = 1000$.

$$\boldsymbol{b} \cdot \boldsymbol{n}(\boldsymbol{x}_i) = B_i(\boldsymbol{x}_i) + \boldsymbol{b} \cdot \boldsymbol{n}(\boldsymbol{x}_{i,0}),$$

provided that the unknown scalar constants $\boldsymbol{b} \cdot \boldsymbol{n}(\boldsymbol{x}_{\mathrm{i},0})$ have been defined. Recall that the boundary scalar field $\boldsymbol{b} \cdot \boldsymbol{n}$ must satisfy the compatibility constraint (5). Incorporating the normal velocity component as defined above yields

$$\sum_{i=1}^{N} \iint_{\Gamma_i} (B_i(\boldsymbol{x}_i) + \boldsymbol{b} \cdot \boldsymbol{n}(\boldsymbol{x}_{i,0}))\, \mathrm{d}\Gamma = D_{\mathrm{in}},$$

where the inlet mass flux D_{in} is assumed to be known. Rearranging this equation yields the following linear combination:

$$\sum_{i=1}^{N} \alpha_i\, \boldsymbol{b} \cdot \boldsymbol{n}(\boldsymbol{x}_{i,0}) = c,$$

where the coefficient α_i denotes the area of the corresponding boundary surfaces Γ_i, and c is some constant depending on the inlet mass flux and the tangential derivatives of the normal velocity component on the boundaries Γ_i. For the sake of simplicity (see below), this equation is rewritten in the following form:

$$\boldsymbol{b} \cdot \boldsymbol{n}(\boldsymbol{x}_{N,0}) = \mathscr{F}(\boldsymbol{b} \cdot \boldsymbol{n}(\boldsymbol{x}_{1,0}), \ldots, \boldsymbol{b} \cdot \boldsymbol{n}(\boldsymbol{x}_{N-1,0})) + C, \tag{23}$$

where the function $\mathscr{F}$ expresses a linear combination of the $N-1$ scalar values $\{\boldsymbol{b} \cdot \boldsymbol{n}(\boldsymbol{x}_{\mathrm{i},0})\}_{i=1,\ldots,N-1}$, and $C = c/\alpha_N$.

As a matter of fact, the definition of the BCs reduces to the determination of the N scalar unknowns $\boldsymbol{b} \cdot \boldsymbol{n}(\boldsymbol{x}_{i,0})$. Each of these specifies the mass flux across the corresponding open boundary part Γ_i. In some particular cases, it may be relevant to enforce these mass fluxes, but from a physical point of view, it is generally more natural to enforce the mean value of the pressure at each outlet. Indeed, in many practical situations, the unknown outflow mass rate across each boundary is depending on the pressure which may be enforced. As outlined by Heywood *et al.* [7], the N conditions for the mass fluxes can then be replaced by

$$\frac{1}{\alpha_i}\iint_{\Gamma_i} p_t \, \mathrm{d}\Gamma \equiv L_i p_t = P_i, \quad i = 1, \ldots, N,$$

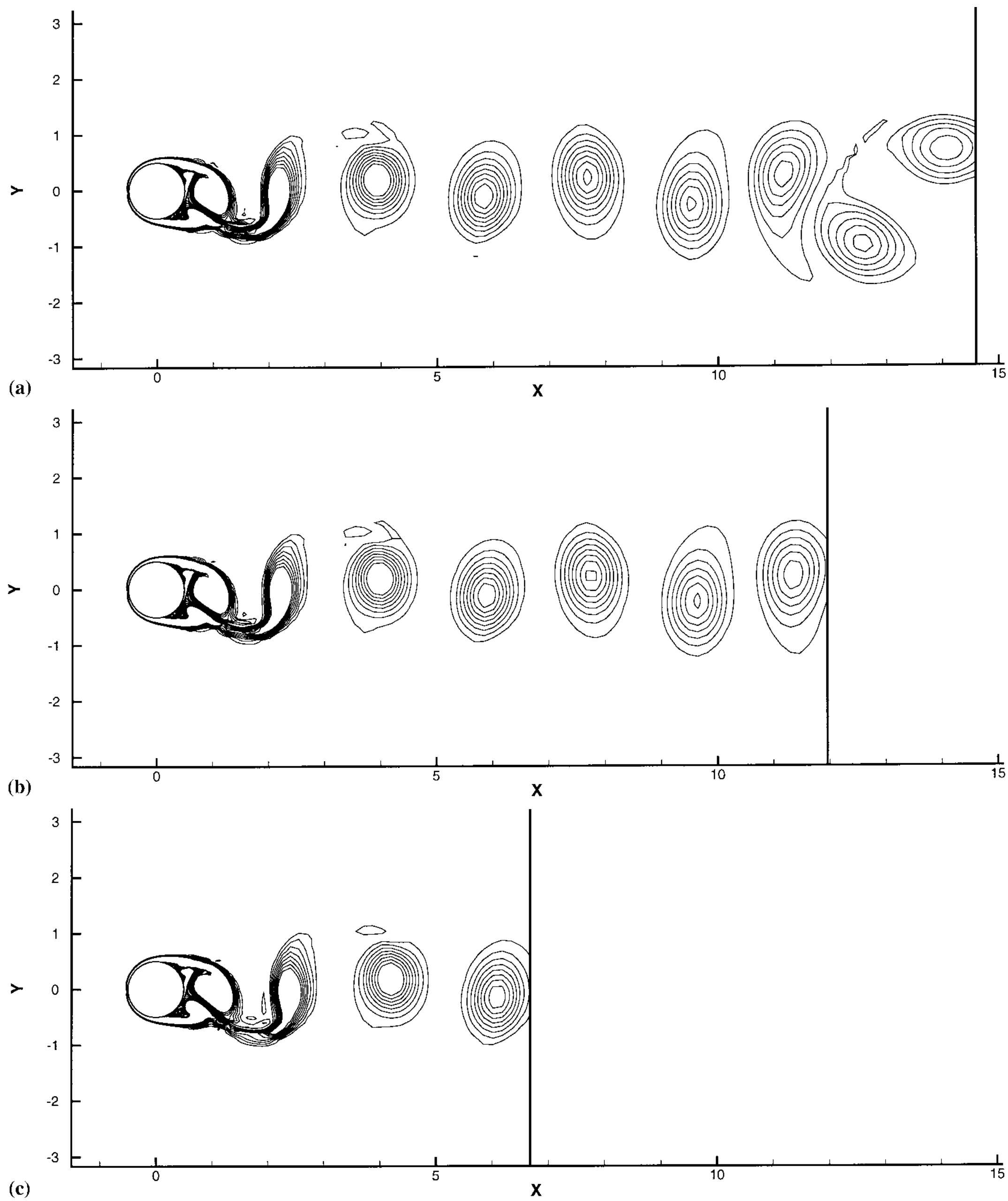

Figure 6. Isovalues of the vorticity, $\Delta w = 0.5$, $Re = 1000$: (a) mesh M2, (b) mesh M3, (c) mesh M4.

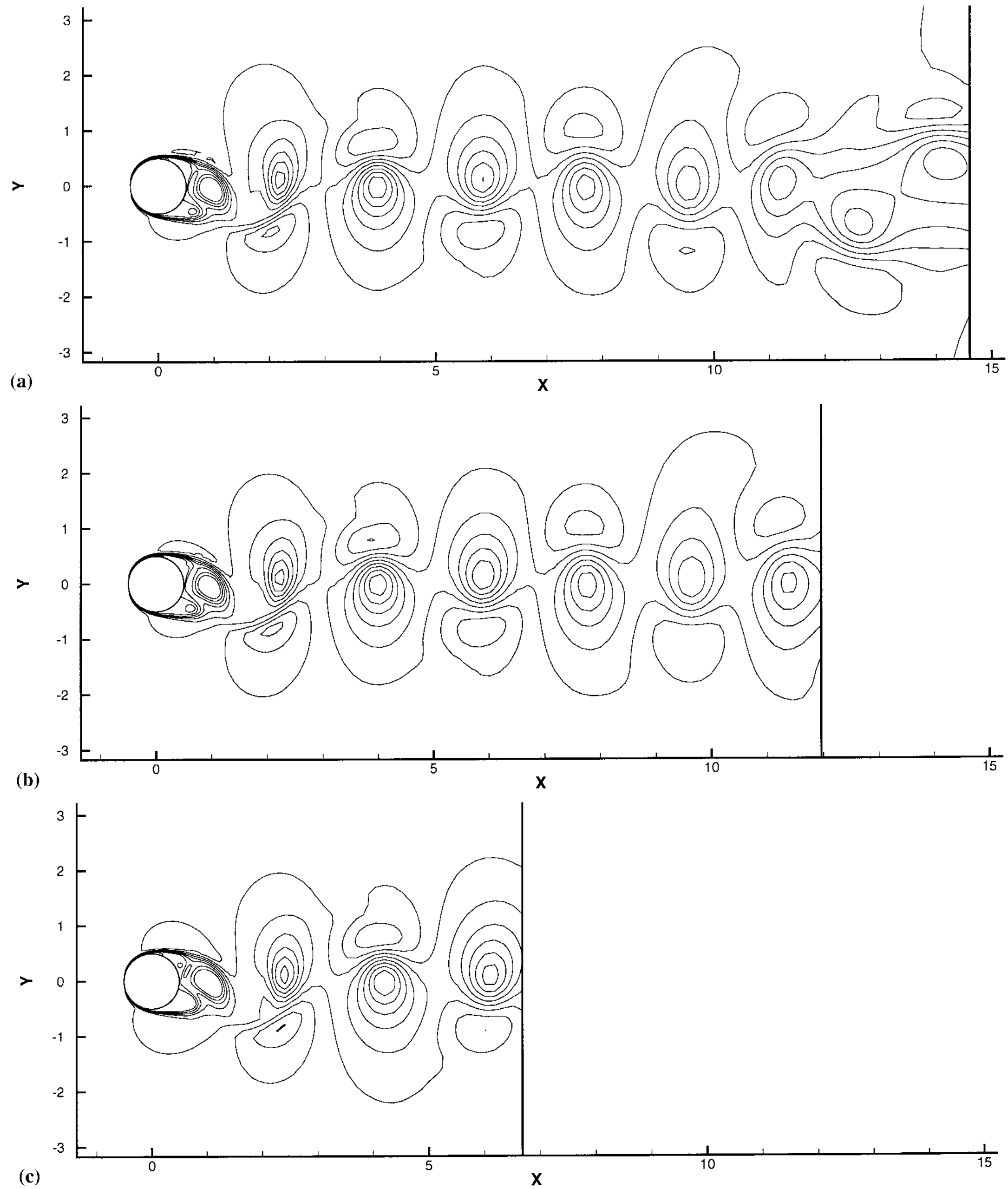

Figure 7. Isovalues of the dynamic pressure, $\Delta p_t = 0.2$, $Re = 1000$: (a) mesh M2, (b) mesh M3, (c) mesh M4.

where L_i denotes the scalar averaging operator on Γ_i, and P_i is some prescribed value of the averaged pressure on the surface Γ_i. It must be emphasized that the pressure is defined up to an arbitrary constant. Consequently, only the difference of the pressure between two open boundaries is significant. The $N-1$ following conditions finally remain:

$$L_i p_t - L_{i+1} p_t = \Delta P_i = P_i - P_{i+1}, \quad i = 1, \ldots, N-1. \tag{24}$$

The compatibility constraint under the form of Equation (23) yields the last equation such that the number of conditions to be enforced equals the number of the unknowns $\{\boldsymbol{b}\cdot\boldsymbol{n}(\boldsymbol{x}_{i,0})\}_{i=1,\ldots,N}$. Notice that the prescribed pressure differences ΔP_i can be time-dependent. It must also be noted that the dynamic pressure, instead of the static one, has here been used due to the rotational form of the Navier–Stokes equations in (1).

5.2. Enforcing the pressure differences

We now describe how the pressure differences can be enforced. The boundary pressure is a function of the velocity component normal to the boundary. Since the definition of this normal component is only required when solving the second step of the Navier–Stokes procedure (i.e. the div–curl problem, see Section 3), the pressure differences have to be enforced only when solving the kinematic problem. As a consequence, the following corrector step must be solved:

$$[A]\quad \begin{cases} \nabla\cdot\boldsymbol{v}=0 & \text{in } \Omega,\\ \nabla\times\boldsymbol{v}=\boldsymbol{w} & \text{in } \Omega,\\ \boldsymbol{v}\cdot\boldsymbol{n}=\boldsymbol{b}\cdot\boldsymbol{n} & \text{on } \Gamma,\\ \boldsymbol{b}\cdot\boldsymbol{n}(\boldsymbol{x}_i)=B_i(\boldsymbol{x}_i)+\boldsymbol{b}\cdot\boldsymbol{n}(\boldsymbol{x}_{i,0}) & \text{on } \Gamma_i,\quad i=1,\ldots,N,\\ \boldsymbol{b}\cdot\boldsymbol{n}(\boldsymbol{x}_{i,0}) \text{ given such that } L_ip_t-L_{i+1}p_t=\Delta P_i & i=1,\ldots,N-1,\\ \boldsymbol{b}\cdot\boldsymbol{n}(\boldsymbol{x}_{N,0})=\mathscr{F}(\boldsymbol{b}\cdot\boldsymbol{n}(\boldsymbol{x}_{1,0}),\ldots,\boldsymbol{b}\cdot\boldsymbol{n}(\boldsymbol{x}_{N-1,0}))+C, & \end{cases}$$

where the vorticity vector field $\boldsymbol{w}$, the constant C, and the $\{B_i(\boldsymbol{x}_i)\}_{i=1,\ldots,N}$ have previously been calculated when solving the dynamic problem (predictor step). It is obvious that the problem [A] is well posed since the compatibility constraint is ensured thanks to the last equation. Introducing the Helmholtz decomposition (15) yields the following Poisson problem for the dynamic pressure field (i.e. ϕ, see Section 3):

$$[P]\quad \begin{cases} \boldsymbol{v}=\tilde{\boldsymbol{v}}-\dfrac{2\,\Delta t}{3}\nabla\phi \quad \text{in } \Omega,\\ \nabla^2\phi=\dfrac{3}{2\,\Delta t}\nabla\cdot\tilde{\boldsymbol{v}} \quad \text{in } \Omega,\\ \nabla\phi\cdot\boldsymbol{n}=\dfrac{3}{2\,\Delta t}(\boldsymbol{v}\cdot\boldsymbol{n}-\boldsymbol{b}\cdot\boldsymbol{n}) \quad \text{on } \Gamma,\\ \boldsymbol{b}\cdot\boldsymbol{n}(\boldsymbol{x}_i)=B_i(\boldsymbol{x}_i)+\boldsymbol{b}\cdot\boldsymbol{n}(\boldsymbol{x}_{i,0}) \quad \text{on } \Gamma_i,\quad i=1,\ldots,N,\\ \boldsymbol{b}\cdot\boldsymbol{n}(\boldsymbol{x}_{i,0}) \text{ given such that } L_ip_t-L_{i+1}p_t=\Delta P_i \quad i=1,\ldots,N-1,\\ \boldsymbol{b}\cdot\boldsymbol{n}(\boldsymbol{x}_{N,0})=\mathscr{F}(\boldsymbol{b}\cdot\boldsymbol{n}(\boldsymbol{x}_{1,0}),\ldots,\boldsymbol{b}\cdot\boldsymbol{n}(\boldsymbol{x}_{N-1,0}))+C, \end{cases}$$

where the predicted vector field $\tilde{\boldsymbol{v}}$ is explicitly given by Equation (12). The only remaining difficulty is to define the correct mass flux on each open boundary in order to satisfy the desired pressure differences.

Taking advantage of the linearity of the above problem with respect to the $\boldsymbol{b}\cdot\boldsymbol{n}(\boldsymbol{x}_{i,0})$, the solution procedure makes use of an influence matrix technique. First, let $\{\overline{\boldsymbol{b}\cdot\boldsymbol{n}}(\boldsymbol{x}_{i,0})\}_{i=1,\ldots,N-1}$ be any arbitrary distribution of the $N-1$ corresponding scalar quantities $\boldsymbol{b}\cdot\boldsymbol{n}(\boldsymbol{x}_{i,0})$ and let us solve the following problem:

$$
[\bar{P}]\quad \begin{cases} \nabla^2\bar{\phi} = \dfrac{3}{2\,\Delta t}\,\nabla\cdot\tilde{\boldsymbol{v}} & \text{in } \Omega,\\[2mm] \nabla\bar{\phi}\cdot\boldsymbol{n} = \dfrac{3}{2\,\Delta t}\,(\tilde{\boldsymbol{v}}\cdot\boldsymbol{n} - \overline{\boldsymbol{b}\cdot\boldsymbol{n}}) & \text{on } \Gamma,\\[2mm] \overline{\boldsymbol{b}\cdot\boldsymbol{n}}(\boldsymbol{x}_i) = B_i(\boldsymbol{x}_i) + \overline{\boldsymbol{b}\cdot\boldsymbol{n}}(\boldsymbol{x}_{i,0}) & \text{on } \Gamma_i, \quad i = 1, \ldots, N\\[2mm] \overline{\boldsymbol{b}\cdot\boldsymbol{n}}(\boldsymbol{x}_{N,0}) = \mathscr{F}(\overline{\boldsymbol{b}\cdot\boldsymbol{n}}(\boldsymbol{x}_{1,0}), \ldots, \overline{\boldsymbol{b}\cdot\boldsymbol{n}}(\boldsymbol{x}_{N-1,0})) + C, & \end{cases}
$$

where $\overline{\boldsymbol{b}\cdot\boldsymbol{n}} = \boldsymbol{b}\cdot\boldsymbol{n}$ everywhere but on Γ_i. As mentioned above, this last problem clearly has a unique solution since it corresponds to a Poisson problem with Neumann BC for which the compatibility constraint is ensured. Owing to the superposition principle for linear problems, the difference between the solution of the original problem $[P]$ and the solution of the above problem $[\bar{P}]$ is sought as a linear combination of the $N-1$ following homogeneous problems:

$$
[\hat{P}^k]\quad \begin{cases} \nabla^2\hat{\phi}^k = 0 & \text{in } \Omega,\\[2mm] \nabla\hat{\phi}^k\cdot\boldsymbol{n} = -\dfrac{3}{2\,\Delta t}\,\widehat{\boldsymbol{b}\cdot\boldsymbol{n}^k} & \text{on } \Gamma,\\[2mm] \widehat{\boldsymbol{b}\cdot\boldsymbol{n}^k}(\boldsymbol{x}_i) = \widehat{\boldsymbol{b}\cdot\boldsymbol{n}^k}(\boldsymbol{x}_{i,0}) & \text{on } \Gamma_i, \quad i = 1, \ldots, N,\\ \widehat{\boldsymbol{b}\cdot\boldsymbol{n}^k}(\boldsymbol{x}_{N,0}) = \mathscr{F}(\widehat{\boldsymbol{b}\cdot\boldsymbol{n}^k}(\boldsymbol{x}_{1,0}), \ldots, \widehat{\boldsymbol{b}\cdot\boldsymbol{n}^k}(\boldsymbol{x}_{N-1,0})), & \\ \widehat{\boldsymbol{b}\cdot\boldsymbol{n}^k}(\boldsymbol{x}_{i,0}) = \delta_i^k & i = 1, \ldots, N-1, \end{cases}
$$

for $k = 1$ to $N-1$, where $\widehat{\boldsymbol{b}\cdot\boldsymbol{n}^k} = 0$ everywhere but on Γ_i, and δ_i^k is the Kronecker symbol. The solution $(\phi, \{\boldsymbol{b}\cdot\boldsymbol{n}(\boldsymbol{x}_i)\}_{i=1,\ldots,N})$ of the problem $[P]$ can thus be expressed as the following linear combination:

$$
\phi = \bar{\phi} + \sum_{k=1}^{N-1} \lambda^k \hat{\phi}^k,
$$

$$
\boldsymbol{b}\cdot\boldsymbol{n}(\boldsymbol{x}_i) = \overline{\boldsymbol{b}\cdot\boldsymbol{n}}(\boldsymbol{x}_i) + \sum_{k=1}^{N-1} \lambda^k \widehat{\boldsymbol{b}\cdot\boldsymbol{n}^k}(\boldsymbol{x}_i), \quad i = 1, \ldots, N,
$$

for which the $N-1$ coefficients λ^k are defined such that the pressure differences (24) are satisfied

$$
L_i\bar{\phi} - L_{i+1}\bar{\phi} + \sum_{k=1}^{N-1} \lambda^k (L_i\hat{\phi}^k - L_{i+1}\hat{\phi}^k) = \Delta P_i, \quad i = 1, \ldots, N-1.
$$

These last equations can be recast in matrix form as

$$
\boldsymbol{M}\cdot\boldsymbol{\lambda} = \boldsymbol{s},
$$

where $\boldsymbol{\lambda} = (\{\lambda^k\}_{k=1,\ldots,N-1})^T$, the elements of the matrix $\boldsymbol{M}$ are

$$
M_{ik} = L_i\hat{\phi} - L_{i+1}\hat{\phi}^k, \quad i = 1, \ldots, N-1; \quad k = 1, \ldots, N-1,
$$

and the elements of the vector $\boldsymbol{s}$ are defined by

$$
s_i = \Delta P_i - L_i\bar{\phi} + L_{i+1}\bar{\phi}, \quad i = 1, \ldots, N-1.
$$

It can be proven that the matrix $\boldsymbol{M}$ is invertible since the problems $[\hat{P}^k]$ have a unique solution.

To sum up, the solution procedure is

- In a preliminary stage:
  - Solve the $N-1$ homogeneous problems $[\hat{P}^k]$.
  - Calculate the residuals $L_i\hat{\phi}^k - L_{i+1}\hat{\phi}^k$.
  - Build the matrix $\boldsymbol{M}$ formed by those residuals, and invert.
- At each time level of the integration of the Navier–Stokes equations:
  - Choose the $\{\overline{\boldsymbol{b}\cdot\boldsymbol{n}}(\boldsymbol{x}_{i,0})\}_{i=1,\ldots,N-1}$ arbitrarily.
  - Solve $[\bar{P}]$ and calculate the residuals $L_i\bar{\phi} - L_{i+1}\bar{\phi}$, then $\boldsymbol{s}$.
  - Multiply by the inverse matrix $\boldsymbol{M}^{-1}$ to obtain the λ^k.
  - Solve the final problem $[P]$ with the corrected scalar data

$$\boldsymbol{b}\cdot\boldsymbol{n}(\boldsymbol{x}_{i,0}) = \overline{\boldsymbol{b}\cdot\boldsymbol{n}}(\boldsymbol{x}_{i,0}) + \lambda^i, \quad i = 1, \ldots, N-1.$$

In this case, the influence matrix only depends on the geometry of the domain (see the problems $[\hat{P}^k]$). This matrix only needs to be calculated at the beginning of the computation, assuming that the mesh remains the same throughout the computation. Moreover, the size of this matrix is proportional to the number of open boundaries N. Hence, except in some special cases, the size of this matrix is small and its inversion will be cheap.

However, the influence matrix technique is based on an exact solution of the operators involved in the initial problem (i.e. the Poisson problem in this case). Numerical inaccuracies in solving those equations may yield large errors in the computed results. When using iterative methods for solving those equations, a great computational time may thus be required in order to minimize these errors.

5.3. Numerical tests

In order to test our approach, the three-dimensional flow inside a branching channel is computed. This channel contains one inlet, and two branches emerging onto two open

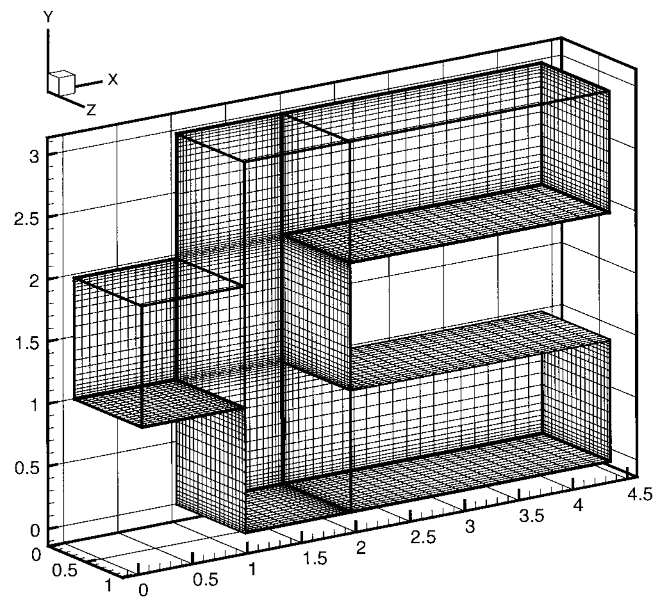

Figure 8. Partial view of the mesh in the branching channel.

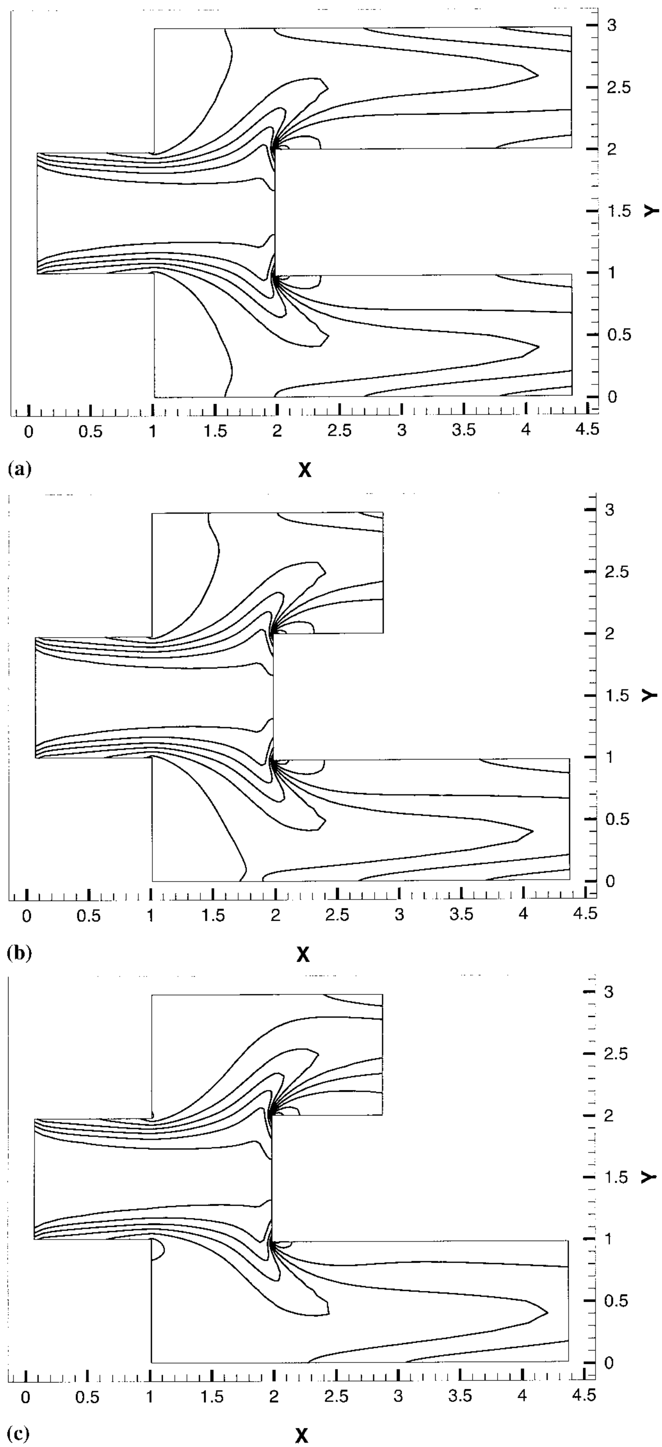

Figure 9. Isovalues of the dynamic pressure in the plane $z = 0.5$, $\Delta p_t = 0.25$: (a) symmetrical case, equal outlet pressures; (b) non-symmetrical case, adjusted outlet pressures; (c) non-symmetrical case, equal outlet pressures.

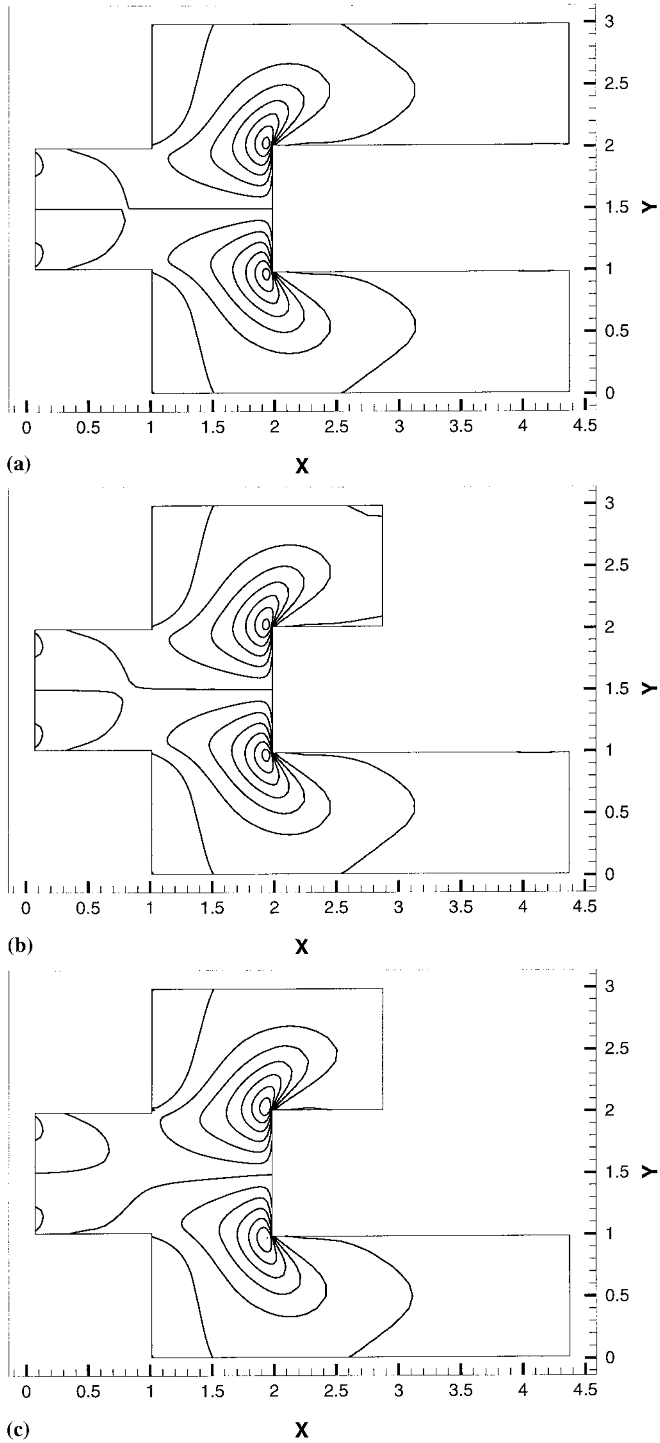

Figure 10. Isovalues of the y component of the velocity in the plane $z = 0.5$, $\Delta v_y = 0.2$: (a) symmetrical case, equal outlet pressures; (b) non-symmetrical case, adjusted outlet pressures; (c) non-symmetrical case, equal outlet pressures.

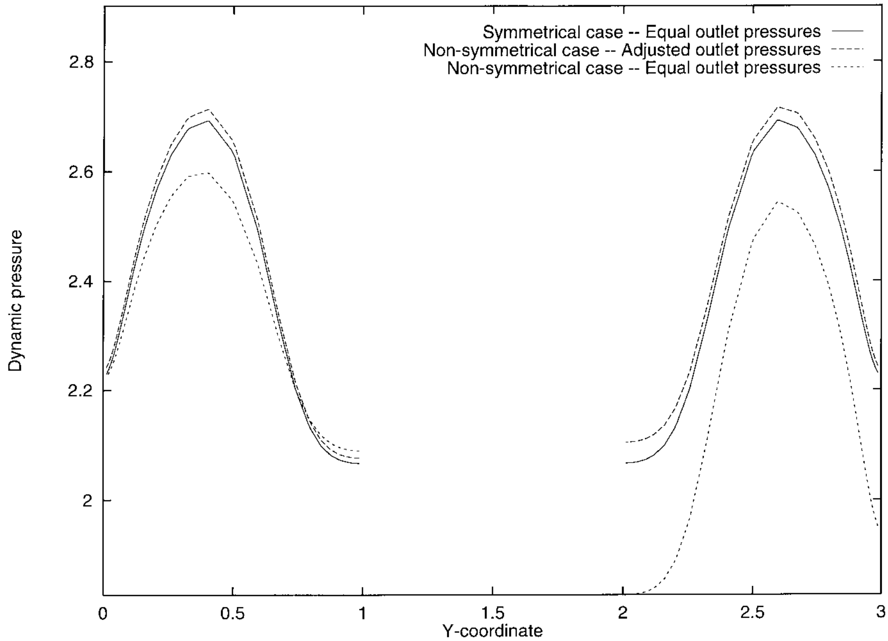

Figure 11. Dynamic pressure along a vertical line in the cross-section plane $x = 2.75$.

boundaries respectively. The computational domain depicted in Figure 8 is symmetrical about the plane $y = 1.5$, where y denotes the vertical direction. z denotes the horizontal direction perpendicular to the main flow direction, and the x-direction is orientated from the inlet to the outlets along the main flow direction. The Reynolds number of the flow based on the width of the channel and the inlet velocity is equal to $Re = 200$.

In the first computational case, the two branches of the channel have the same length and equal (dynamic) pressures are enforced at both outlets. The flow field is thus expected to be symmetrical with respect to the above-mentioned symmetry plane, as it can be seen from the isocontours on the centre plane $z = 0.5$ of the dynamic pressure (Figure 9(a)) and of the y component of the velocity (Figure 10(a)) at the dimensionless time $t = 5$.

In the second case, the upper branch is cut such that the computational domain is no longer symmetrical. Zero pressure difference between the two outlets is also enforced. As could be expected, the flow field becomes now non-symmetrical (see Figures 9(c) and 10(c)).

Finally, the averaged pressure difference between the cut-plane and the other non-truncated outlet can be extracted in the course of the symmetrical computation. The 'adjusted' pressure difference can then be enforced as a BC when solving the flow on the non-symmetrical domain. It is expected that the flow becomes symmetrical again. Indeed, Figures 9(b) and 10(b) exhibit a very good agreement with the results of the symmetrical computation on Figures 9(a) and 10(a).

These results are corroborated by a profile plot for the dynamic pressure in the cross-section plane $x = 2.75$, which is located just upstream the cut-plane, along a vertical line in the centre plane of the channel (Figure 11). Once again, the flow is found to be symmetrical when the computation is symmetrical, or when the pressure difference is adjusted for the non-symmetrical domain; whereas it is unsymmetrical if the averaged pressures are set equal at both outlets and when the domain is not symmetrical.

6. EXTENSION TO A FRACTIONAL STEP METHOD

As shown in Section 3.2, the methodology used for solving the $\boldsymbol{v}-\boldsymbol{w}$ formulation of the Navier–Stokes equations is readily equivalent to a fractional step method. Therefore, the methods that have been proposed above for solving both the OBCs and the case of several open boundaries can be used in this context. However, some particular points have to be emphasized.

First, it has been mentioned already that the two methods are equivalent provided that BCs are strictly the same. Consequently, Neumann BCs should be enforced for the tangential components of the velocity in the predictor step, arising from the Dirichlet BCs for the tangential vorticity components.

Second, most of the authors dealing with the Navier–Stokes equations in primitive variables make use of the following formulation:

$$\frac{\partial \boldsymbol{v}}{\partial t} + (\boldsymbol{v}\cdot\nabla)\boldsymbol{v} = -\nabla p + \frac{1}{Re}\nabla^2\boldsymbol{v}.$$

Concerning the convective term, both the rotational form of Equation (1) and the latter form are possible. However, in this last case we have to deal with the static pressure p. Thus, the pressure differences in Section 5 will involve the static pressure instead of the dynamic one. Let us now concentrate on the viscous term. The Laplace vector operator is equivalent to the double curl operator by virtue of the divergence-free condition and of the following relationship:

$$\nabla^2\boldsymbol{v} = \nabla(\nabla\cdot\boldsymbol{v}) - \nabla\times\nabla\times\boldsymbol{v}. \tag{25}$$

Let us assume that this Laplace operator is used for solving the predictor step of the fractional step method. Recall that the corrector step consists of adding a pressure gradient to the predicted velocity $\tilde{\boldsymbol{v}}$ to obtain the final velocity $\boldsymbol{v}^{n+1}$. The double curl operator allows for the cancellation of this gradient. In other respects, the pressure is calculated such that the final velocity is divergence-free, the first term on the right-hand-side of Equation (25) will thus cancel. Consequently, the momentum equation for the final velocity will be preserved at the end of the corrector step inside the computational domain. Nevertheless, when using the Laplace operator, Dirichlet BCs for the velocity component normal to the boundary are required, in addition with the Neumann BCs for the tangential components of the velocity involved with the double curl operator. As a matter of fact, the predictor step will be dependent on the normal component of the boundary velocity. The influence matrix technique that has been introduced for solving the corrector step, the purpose of which is to define the normal velocity component, is not adapted to handle this coupling between the momentum equation and the incompressibility constraint. This is the reason why the rotational form of the viscous term should be used when dealing with a fractional step method for solving the Navier–Stokes equations in primitive variables in this context. Nevertheless, such a coupling could be taken into account by incorporating the predictor step together with the corrector step into the influence matrix technique.

7. CONCLUSION

In this contribution, two aspects of the solution of the incompressible Navier–Stokes equations were treated. First, OBCs for the equations have been stated. These allow us to accurately enforce the incompressibility constraint, and make use of a non-reflecting wave-like equation for an additional quantity. Second, the case of multiple open boundaries has been considered. An algorithm for splitting the inlet mass flux onto the several open boundaries by enforcing the averaged pressure differences between these boundaries has been proposed. For this purpose, an influence matrix technique is used. In order to facilitate the demonstrations, the Navier–Stokes equations have been recasted in velocity–vorticity formulation. However, both methodologies can formally be extended to a particular fractional step method, for which BCs and forms of the viscous term are not commonly used by people who have dealt with such methods. It has also been numerically proven that these methodologies are effective when dealing with domains with one or several open boundaries.

ACKNOWLEDGMENTS

The author is especially grateful to Ta Phuoc Loc for fruitful discussions and useful advice. R. Lardat is also acknowledged for the collaboration in the early stage of this study. This work was financially supported by a co-sponsored BDI funding from the Centre National de la Recherche Scientifique and the Centre National d'Etudes Spatiales during the first period of this work, as well as by a grant from Risø National Laboratory in the second period.

REFERENCES

1. F. Bertagnolio and R. Lardat, 'Open boundary conditions for the incompressible Navier–Stokes equations in velocity–vorticity form', in C. Taylor (ed.), *Proceedings of the 10th International Conference on Numerical Methods for Laminar and Turbulent Flow*, Pineridge Press, Swansea, UK, 1997.
2. R.L. Sani and P.M. Gresho, 'Résumé and remarks on the open boundary condition mini-symposium', *Int. J. Numer. Methods Fluids*, **18**, 983–1008 (1994).
3. W. Shyy, 'Numerical outflow boundary conditions for Navier–Stokes flow calculations by a line iterative method', *AIAA J.*, **23**, 1847–1848 (1985).
4. M. Behr, J. Liou, R. Shih and T.E. Tezduyar, 'Vorticity–streamfunction formulation of unsteady incompressible flow past a cylinder: sensitivity of the computed flow field to the location of the outflow boundary', *Int. J. Numer. Methods Fluids*, **12**, 323–342 (1991).
5. P.M. Gresho, 'Incompressible fluid dynamics: some fundamental formulation issues', *Annu. Rev. Fluid Mech.*, **23**, 413–453 (1991).
6. Ch.-H. Bruneau and P. Fabrie, 'Effective downstream boundary conditions for incompressible Navier–Stokes equations', *Int. J. Numer. Methods Fluids*, **19**, 693–705 (1994).
7. J.G. Heywood, R. Rannacher and S. Turek, 'Artificial boundaries and flux and pressure conditions for the incompressible Navier–Stokes equations', *Int. J. Numer. Methods Fluids*, **22**, 325–352 (1996).
8. T.P. Loc and R. Bouard, 'Numerical solution of the early stage of the unsteady viscous flow around a circular cylinder: a comparison with experimental visualization and measurements', *J. Fluid Mech.*, **160**, 93–117 (1985).
9. J.N. Sørensen and T.P. Loc, 'Inflow and outflow boundary conditions for incompressible, axisymmetric flows', in C. Taylor, P.M. Gresho, R.L. Sani and J. Haüser (eds.), *Proceedings of the 6th International Conference on Numerical Methods in Laminar and Turbulent Flow*, Pineridge Press, Swansea, UK, 1989.
10. W.E. Liu and J.G. Liu, 'Vorticity boundary condition and related issues for finite difference schemes', *J. Comput. Phys.*, **124**, 368–382 (1996).
11. R. Lardat, F. Bertagnolio and O. Daube, 'La formulation vitesse–tourbillon en maillage decale: une methode de projection', *C.R. Acad. Sci. Paris, Sér. II b*, **324**, 747 (1997).
12. O. Daube, J.L. Guermond and A. Sellier, 'Sur la formulation vitesse–tourbillon des équations de Navier–Stokes en ecoulement incompressible', *C.R. Acad. Sci. Paris, Sér. II*, **313**, 377–382 (1991).
13. S.C.R. Dennis and L. Quartapelle, 'Direct solution of the vorticity–streamfunction ordinary differential equations by a Chebyshev approximation', *J. Comput. Phys.*, **52**, 448 (1983).
14. O. Daube, 'Resolution of the 2D Navier–Stokes equations in velocity–vorticity form by means of an influence matrix', *J. Comput. Phys.*, **103**, 402–414 (1992).
15. J.N. Sørensen and T.P. Loc, 'High-order axisymmetric Navier–Stokes code: description and evaluation of boundary conditions', *Int. J. Numer. Methods Fluids*, **9**, 1517–1537 (1989).
16. F. Bertagnolio and O. Daube, 'Solution of the div–curl problem in generalized curvilinear co-ordinates', *J. Comput. Phys.*, **138**, 121–152 (1997).

17. F. Bertagnolio and O. Daube. 'Three-dimensional incompressible Navier–Stokes equations on non-orthogonal staggered grids using the velocity–vorticity formulation', *Int. J. Numer. Methods Fluids*, **28**, 917–943 (1998).
18. G. Jin and M. Braza, 'A nonreflecting outlet boundary condition for incompressible unsteady Navier–Stokes calculations', *J. Comput. Phys.*, **107**, 239–253 (1993).
19. B. Engquist and N. Majda, 'Numerical radiation boundary conditions for unsteady transonic flow', *J. Comput. Phys.*, **40**, 91–103 (1981).
20. M. Coutanceau and R. Bouard, 'Experimental determination of the main features of the viscous flow in the wake of a circular cylinder', *J. Fluid Mech.*, **79**, 257 (1976).
21. W.M. Collins and S.C.R. Dennis, 'Flow past an impusively started cylinder', *J. Fluid Mech.*, **60**, 105 (1973).
22. C. Liu, X. Zheng and C.H. Sung, 'Preconditioned multigrid methods for unsteady incompressible flows', *J. Comput. Phys.*, **139**, 35–57 (1998).

